

# Top partner production at $e^+e^-$ collider in the littlest Higgs Model with T-parity

Haiyan Wang<sup>1</sup> and Bingfang Yang<sup>1,2\*</sup>

<sup>1</sup> *School of Materials Science and Engineering,  
Henan Polytechnic University, Jiaozuo 454000, China*

<sup>2</sup> *College of Physics and Materials Science,  
Henan Normal University, Xinxiang 453007, China*

## Abstract

In the framework of the littlest Higgs Model with T-parity, we discuss the top partner production at future  $e^+e^-$  collider. We calculate the cross sections of the top partner production processes and associated production processes of Higgs and top partner under current constraints. Then, we investigate the observability of the T-odd top partner pair production through the process  $e^+e^- \rightarrow T_-\bar{T}_- \rightarrow t\bar{t}A_H A_H$  in the  $t\bar{t}$  di-lepton channel for two T-odd top partner mass  $m_{T_-}=603(708)$  GeV at  $\sqrt{s}=1.5$  TeV. We analyze the signal significance depending on the integrated luminosity and find this signal is promising at the future high energy  $e^+e^-$  collider.

PACS numbers: 14.65.Ha,13.66.Hk,12.60.-i

---

\*Electronic address: yangbingfang@htu.edu.cn

## I. INTRODUCTION

The discovery of the Higgs boson at the Large Hadron Collider (LHC) [1] is a great step towards understanding the electroweak symmetry breaking (EWSB) mechanism. However, the little hierarchy problem[2], which is essentially from quadratically divergent corrections to the Higgs mass parameter, still exists. In the past, various new physics models have been proposed to solve this problem, and the littlest Higgs Model with T-parity (LHT) [3] is one of the most promising candidates.

In the LHT model, the Higgs boson is constructed as a pseudo-Nambu-Goldstone particle of the broken global symmetry. The quadratic divergence contributions to Higgs boson mass from the SM top quark loop, gauge boson loops and the Higgs self-energy are cancelled by the corresponding T-parity partners, respectively. Among the partners, the top partner is the most important one since it is responsible for cancelling the largest quadratically divergent correction to the Higgs mass induced by the top quark.

Recently, the ATLAS and CMS collaborations have performed the searches for the vector-like top partner through the pair or single production with three final states  $bW$ ,  $tZ$  and  $tH$ , and have excluded the top partner with the mass less than about 700 GeV [4]. Besides, a search has been performed in pair-produced exotic top partners, each decay to an on-shell top (or antitop) quark and a long-lived undetected neutral particle[5]. Apart from direct searches, the indirect searches for the top partners through their contributions to the electroweak precision observables (EWPOs) [6],  $Z$ -pole observables [7] and the flavor physics [8] have been extensively investigated. The recent research[9] shows that the direct bounds on the heavy vector-like top quarks have been stronger than the indirect constraints. The null results of the top partners, in conjunction with the EWPOs and the recent Higgs data, have tightly constrained the parameter space of the LHT model[10, 11].

Compared to the hadron colliders,  $e^+e^-$  linear colliders may provide cleaner environments to study productions and decays of various particles. Some design schemes have been put forward, such as the International Linear Collider(ILC) [12]and the Compact Linear Collider(CLIC) [13], they can run at the center of mass (c.m.) energy ranged from 500 GeV to 3000 GeV, which enables us to perform precision measurements of the top partner above the threshold. In addition, the polarization of the initial beams at  $e^+e^-$  linear colliders will be useful to study the properties of the top partner. Some relevant

works have been widely studied in various extensions of the Standard Model (SM)[14], including the Little Higgs model[15]. However, the works in Little Higgs model mostly were performed many years ago and before the discovery of the Higgs boson, so it is necessary to revisit this topic. Moreover, the different final states are analyzed in this work.

The paper is organized as follows. In Sec.II we review the top partner in the LHT model. In Sec.III we calculate top partner production cross sections. In Sec.IV we investigate signal and discovery potentiality of the top partner production at  $e^+e^-$  collider. Finally, we draw our conclusions in Sec.V.

## II. TOP PARTNER IN THE LHT MODEL

The LHT model is a non-linear  $\sigma$  model based on the coset space  $SU(5)/SO(5)$ [16]. The global group  $SU(5)$  is spontaneously broken into  $SO(5)$  at the scale  $f \sim \mathcal{O}(\text{TeV})$  by the vacuum expectation value (VEV) of the  $\Sigma$  field, which is given by

$$\Sigma_0 = \langle \Sigma \rangle = \begin{pmatrix} \mathbf{0}_{2 \times 2} & 0 & \mathbf{1}_{2 \times 2} \\ 0 & 1 & 0 \\ \mathbf{1}_{2 \times 2} & 0 & \mathbf{0}_{2 \times 2} \end{pmatrix}. \quad (1)$$

The VEV  $\Sigma_0$  also breaks the gauged subgroup  $[SU(2) \times U(1)]^2$  of  $SU(5)$  down to the diagonal SM electroweak symmetry  $SU(2)_L \times U(1)_Y$ . After the symmetry breaking, there arise 4 new heavy gauge bosons  $W_H^\pm, Z_H, A_H$  whose masses given at  $\mathcal{O}(v^2/f^2)$  by

$$M_{W_H} = M_{Z_H} = gf(1 - \frac{v^2}{8f^2}), \quad M_{A_H} = \frac{g'f}{\sqrt{5}}(1 - \frac{5v^2}{8f^2}) \quad (2)$$

with  $g$  and  $g'$  being the SM  $SU(2)_L$  and  $U(1)_Y$  gauge couplings, respectively. The heavy photon  $A_H$  is the lightest  $T$ -odd particle and can serve as a candidate for dark matter. In order to match the SM prediction for the gauge boson masses, the VEV  $v$  needs to be redefined as

$$v = \frac{f}{\sqrt{2}} \arccos \left( 1 - \frac{v_{\text{SM}}^2}{f^2} \right) \simeq v_{\text{SM}} \left( 1 + \frac{1}{12} \frac{v_{\text{SM}}^2}{f^2} \right), \quad (3)$$

where  $v_{\text{SM}} = 246$  GeV.

In the fermion sector, the implementation of T-parity requires the existence of mirror partners for each original fermion. In order to do this, two fermion  $SU(2)$  doublets  $q_1$  and

$q_2$  are introduced and  $T$ -parity interchanges these two doublets. A  $T$ -even combination of these doublets is taken as the SM fermion doublet and the  $T$ -odd combination is its  $T$ -parity partner. The doublets  $q_1$  and  $q_2$  are embedded into incomplete  $SU(5)$  multiplets  $\Psi_1$  and  $\Psi_2$  as  $\Psi_1 = (q_1, 0, 0_2)^T$  and  $\Psi_2 = (0_2, 0, q_2)^T$ , where  $0_2 = (0, 0)^T$ . To give the additional fermions masses, an  $SO(5)$  multiplet  $\Psi_c$  is also introduced as  $\Psi_c = (q_c, \chi_c, \tilde{q}_c)^T$ , whose transformation under the  $SU(5)$  is non-linear:  $\Psi_c \rightarrow U\Psi_c$ , where  $U$  is the unbroken  $SO(5)$  rotation in a non-linear representation of the  $SU(5)$ . The components of the latter  $\Psi_c$  multiplet are the so-called mirror fermions. Then, one can write down the following Yukawa-type interaction to give masses of the mirror fermions

$$\mathcal{L}_{\text{mirror}} = -\kappa_{ij} f (\bar{\Psi}_2^i \xi + \bar{\Psi}_1^i \Sigma_0 \Omega \xi^\dagger \Omega) \Psi_c^j + h.c. \quad (4)$$

where  $i, j = 1, 2, 3$  are the generation indices. The masses of the mirror quarks  $u_H^i, d_H^i$  and mirror leptons  $l_H^i, \nu_H^i$  up to  $\mathcal{O}(v^2/f^2)$  are given by

$$m_{d_H^i} = \sqrt{2}\kappa_i f, \quad m_{u_H^i} = m_{d_H^i} \left(1 - \frac{v^2}{8f^2}\right), \quad (5)$$

$$m_{l_H^i} = \sqrt{2}\kappa_i f, \quad m_{\nu_H^i} = m_{l_H^i} \left(1 - \frac{v^2}{8f^2}\right), \quad (6)$$

where  $\kappa_i$  are the diagonalized Yukawa couplings.

In the top quark sector, two singlet fields  $T_{L_1}$  and  $T_{L_2}$  (and their right-handed counterparts) are introduced to cancel the large radiative correction to the Higgs mass induced by the top quark. Both fields are embedded together with the  $q_1$  and  $q_2$  doublets into the  $SU(5)$  multiplets:  $\Psi_{1,t} = (q_1, T_{L_1}, 0_2)^T$  and  $\Psi_{2,t} = (0_2, T_{L_2}, q_2)^T$ . The  $T$ -even combination of  $q_i$  is the SM fermion doublet and the other  $T$ -odd combination is its  $T$ -parity partner. Then, the  $T$ -parity invariant Yukawa Lagrangian for the top sector can be written down as follow:

$$\begin{aligned} \mathcal{L}_t = & -\frac{\lambda_1 f}{2\sqrt{2}} \epsilon_{ijk} \epsilon_{xy} \left[ (\bar{\Psi}_{1,t})_i \Sigma_{jx} \Sigma_{ky} - (\bar{\Psi}_{2,t} \Sigma_0)_i \Sigma'_{jx} \Sigma'_{ky} \right] t'_R \\ & - \lambda_2 f (\bar{T}_{L_1} T_{R_1} + \bar{T}_{L_2} T_{R_2}) + h.c. \end{aligned} \quad (7)$$

where  $\epsilon_{ijk}$  and  $\epsilon_{xy}$  are the antisymmetric tensors with  $i, j, k = 1, 2, 3$  and  $x, y = 4, 5$ ,  $\Sigma' = \langle \Sigma \rangle \Omega \Sigma^\dagger \Omega \langle \Sigma \rangle$  is the image of  $\Sigma$  under  $T$ -parity,  $\lambda_1$  and  $\lambda_2$  are two dimensionless top quark Yukawa couplings. Under  $T$ -parity, these fields transform as:  $T_{L_1} \leftrightarrow -T_{L_2}$ ,

$T_{R_1} \leftrightarrow -T_{R_2}$ ,  $t'_R \rightarrow t'_R$ . The above Lagrangian contains the following mass terms:

$$\mathcal{L}_t \supset -\lambda_1 f \left( \frac{s_\Sigma}{\sqrt{2}} \bar{t}_{L_+} t'_R + \frac{1+c_\Sigma}{2} \bar{T}'_{L_+} t'_R \right) - \lambda_2 f (\bar{T}'_{L_+} T'_{R_+} + \bar{T}'_{L_-} T'_{R_-}) + \text{h.c.} \quad (8)$$

where  $c_\Sigma = \cos(\sqrt{2}h/f)$  and  $s_\Sigma = \sin(\sqrt{2}h/f)$ . The  $T$ -parity eigenstates have been defined as  $t_{L_+} = (t_{L_1} - t_{R_1})/\sqrt{2}$ ,  $T'_{L_\pm} = (T_{L_1} \mp T_{L_2})/\sqrt{2}$  and  $T'_{R_\pm} = (T_{R_1} \mp T_{R_2})/\sqrt{2}$ . Note that T-odd Dirac fermion  $T_- \equiv (T'_{L_-}, T'_{R_-})$  does not have the tree level Higgs boson interaction, and thus it does not contribute to the Higgs mass at one-loop level.

The two T-even eigenstates  $(t_{L_+}, t'_R)$  and  $(T'_{L_+}, T'_{R_+})$  mix with each other so that the mass eigenstates can be defined as

$$\begin{aligned} t_L &= \cos \beta t_{L_+} - \sin \beta T'_{L_+}, & T_{L_+} &= \sin \beta t_{L_+} + \cos \beta T'_{L_+}, \\ t_R &= \cos \alpha t'_R - \sin \alpha T'_{R_+}, & T_{R_+} &= \sin \alpha t'_R + \cos \alpha T'_{R_+}, \end{aligned} \quad (9)$$

where the mixing angles  $\alpha$  and  $\beta$  can be defined by the dimensionless ratio  $R = \lambda_1/\lambda_2$  as,

$$\sin \alpha = \frac{R}{\sqrt{1+R^2}}, \quad \sin \beta = \frac{R^2}{1+R^2} \frac{v}{f}. \quad (10)$$

The  $t \equiv (t_L, t_R)$  quark is identified with the SM top quark, and  $T_+ \equiv (T_{L_+}, T_{R_+})$  is its T-even heavy partner, which is responsible for the cancellation of the quadratic divergence to the Higgs mass induced by the top quark loop.

The Yukawa term generates the masses of the top quark and its partners, which are given at  $\mathcal{O}(v^2/f^2)$  by

$$\begin{aligned} m_t &= \frac{\lambda_2 v R}{\sqrt{1+R^2}} \left[ 1 + \frac{v^2}{f^2} \left( -\frac{1}{3} + \frac{1}{2} \frac{R^2}{(1+R^2)^2} \right) \right] \\ m_{T_+} &= \frac{f m_t (1+R^2)}{v R} \left[ 1 + \frac{v^2}{f^2} \left( \frac{1}{3} - \frac{R^2}{(1+R^2)^2} \right) \right] \\ m_{T_-} &= \frac{f m_t \sqrt{1+R^2}}{v R} \left[ 1 + \frac{v^2}{f^2} \left( \frac{1}{3} - \frac{1}{2} \frac{R^2}{(1+R^2)^2} \right) \right] \end{aligned} \quad (11)$$

Since the  $T_+$  mass is always larger than the T-odd top partner  $T_-$  mass, the  $T_+$  can decay into  $A_H T_-$  in addition to the conventional decay modes ( $Wb, tZ, tH$ ).

The T-invariant Lagrangians of the Yukawa interactions of the down-type quarks and charged leptons can be constructed by two possible ways, which are denoted as Case A and Case B, respectively[17]. In the two cases, the corrections to the Higgs couplings with

the down-type quarks and charged leptons with respect to their SM values are given at order  $\mathcal{O}(v_{SM}^4/f^4)$  by ( $d \equiv d, s, b, \ell_i^\pm$ )

$$\begin{aligned} \frac{g_{h\bar{d}d}}{g_{h\bar{d}d}^{SM}} &= 1 - \frac{1}{4} \frac{v_{SM}^2}{f^2} + \frac{7}{32} \frac{v_{SM}^4}{f^4} && \text{Case A} \\ \frac{g_{h\bar{d}d}}{g_{h\bar{d}d}^{SM}} &= 1 - \frac{5}{4} \frac{v_{SM}^2}{f^2} - \frac{17}{32} \frac{v_{SM}^4}{f^4} && \text{Case B} \end{aligned} \quad (12)$$

### III. TOP PARTNER PRODUCTION IN $e^+e^-$ COLLISION

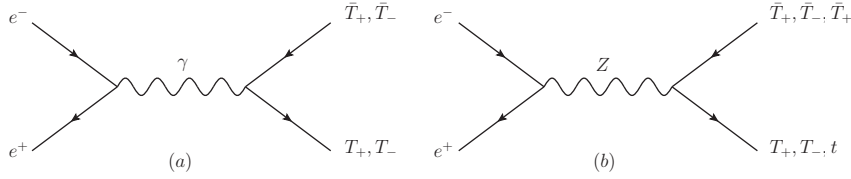


FIG. 1: Feynman diagrams of the top partner production at  $e^+e^-$  collider.

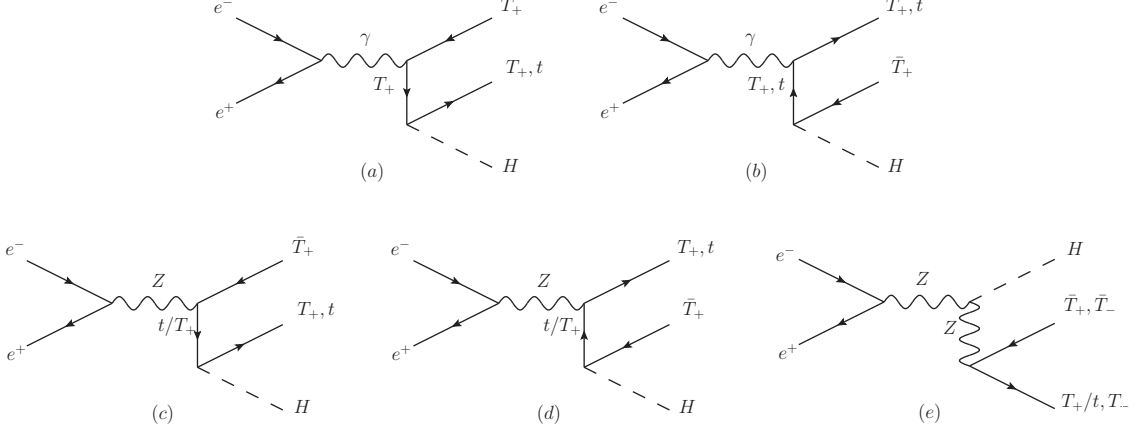


FIG. 2: Feynman diagrams of the Higgs and top partner associated production at  $e^+e^-$  collider.

In the LHT model, the Feynman diagrams of top partner production are shown in Fig.1, which proceeds through the  $s$ -channel  $\gamma$  and  $Z$  exchange diagrams. These processes include T-even top partner pair production  $e^+e^- \rightarrow T_+\bar{T}_+$ , T-odd top partner pair production  $e^+e^- \rightarrow T_-\bar{T}_-$  and a T-even top partner associating with a top quark production  $e^+e^- \rightarrow t\bar{T}_+$ .

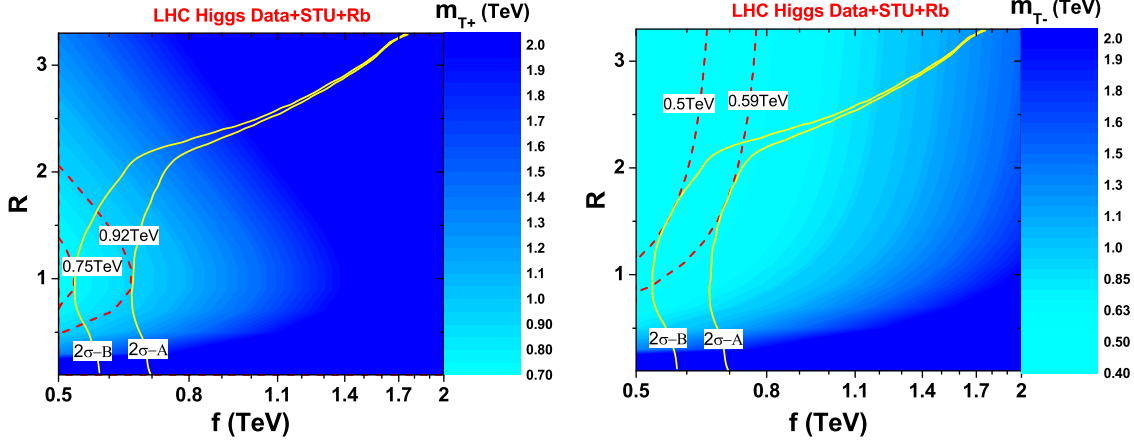


FIG. 3: Exclusion limits on the top partner masses on the  $R \sim f$  plane at  $2\sigma$  confidence level for Case A and Case B, where the parameter  $\kappa$  is marginalized over.

The Feynman diagrams of the Higgs and top partner associated production are shown in Fig.2, which has additional diagrams mediated by the T-even top partner  $T_+$  compared to the process  $e^+e^- \rightarrow t\bar{t}H$  in the SM. These processes include Higgs associating with T-even top partner pair production  $e^+e^- \rightarrow T_+\bar{T}_+H$ , Higgs associating with T-odd top partner pair production  $e^+e^- \rightarrow T_-\bar{T}_-H$  and Higgs associating with a top quark and a T-even top partner production  $e^+e^- \rightarrow t\bar{T}_+H$ .

Before calculating the top partner production cross section, we firstly consider the constraints on the top partner mass from current measurements. We update the constraint on the LHT parameter in our previous works[18], where the global fit of the latest Higgs data, EWPOs and  $R_b$  measurements is performed. Thereinto, the constraints from the direct searches for Higgs data at Tevatron [19][20]and LHC[21][22] are obtained by the package HiggsSignals-1.4.0[23], which is linked to the HiggsBounds-4.2.1[24] library. We compute the  $\chi^2$  values by the method introduced in Ref.[25] and obtained the constraint on the LHT parameter space. This constraint will lead to the exclusion limits on the top partner masses, which is displayed on the  $R \sim f$  plane for Case A and Case B in Fig.3 at  $2\sigma$  confidence level with  $\delta\chi^2 = 8.02$ . We can see that the combined constraints can respectively exclude  $m_{T_+}$  and  $m_{T_-}$  up to

$$m_{T_+} > 920(750)\text{GeV} \quad \text{Case A(B)}, \quad (13)$$

$$m_{T_-} > 590(500)\text{GeV} \quad \text{Case A(B)}. \quad (14)$$

One can notice that Case B predicts a stronger suppression for the down-type fermion couplings to the Higgs boson, such as  $Hb\bar{b}$ , which helps to enhance the branching ratios of  $H \rightarrow \gamma\gamma, WW^*, ZZ^*, \tau\tau$ , so that the Case B is favored by the experimental data[26].

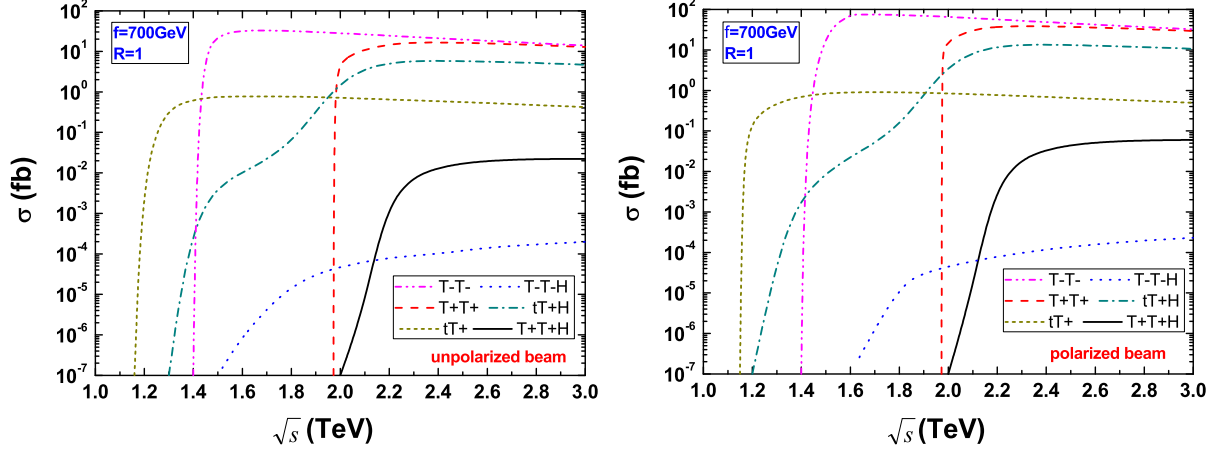


FIG. 4: Top partner production cross sections as a function of  $\sqrt{s}$  for  $f = 700\text{GeV}$ ,  $R = 1$  in  $e^+e^-$  collision with (un)polarized beam.

In the left frame of Fig.4, we show the top partner production cross sections as a function of c.m. energy  $\sqrt{s}$  for  $f = 700\text{ GeV}$ ,  $R = 1$  (correspond to  $m_{T_+} = 986\text{ GeV}$  and  $m_{T_-} = 708\text{ GeV}$ ) in  $e^+e^-$  collision with unpolarized beams. The production cross sections are calculated at tree-level by using CalcHEP 3.6.25[27], where the SM parameters are taken as follows[28]

$$\sin^2 \theta_W = 0.231, \alpha_e = 1/128, M_Z = 91.1876\text{GeV}, m_t = 173.5\text{GeV}, m_H = 125\text{GeV}.$$

We can see that the top partner pair production cross sections increase abruptly at threshold, reaches a maximum roughly 200 GeV above threshold. Then, the production cross sections fall roughly with the c.m. energy  $\sqrt{s}$  increase due to the  $s$ -channel suppression. The  $T_-\bar{T}_-$  production usually has a larger cross section than  $T_+\bar{T}_+$  production since the  $T_-$  mass is always lighter than the  $T_+$  mass in the LHT model. The production cross sections of the associated production of Higgs and top partner have the similar behavior as the top partner pair production, but usually have smaller cross sections due to smaller phase space. The production cross section of the process  $e^+e^- \rightarrow t\bar{T}_+H$  reaches its maximum when the resonance decay of the top partner  $T_+$  emerges.



Considering the polarization of the initial electron and positron beams, the cross section at  $e^+e^-$  collider can be expressed as[29]

$$\begin{aligned} \sigma = \frac{1}{4} & [(1 + p_e)(1 + p_{\bar{e}})\sigma_{RR} + (1 - p_e)(1 - p_{\bar{e}})\sigma_{LL} \\ & + (1 + p_e)(1 - p_{\bar{e}})\sigma_{RL} + (1 - p_e)(1 + p_{\bar{e}})\sigma_{LR}], \end{aligned} \quad (15)$$

where  $\sigma_{RL}$  is the cross section for completely right-handed polarized  $e^-$  beam ( $p_e = +1$ ) and completely left-handed polarized  $e^+$  beam ( $p_{\bar{e}} = -1$ ), and other cross sections  $\sigma_{RR}$ ,  $\sigma_{LL}$  and  $\sigma_{LR}$  are defined analogously. We show the top partner production cross sections in polarized beam with  $p_e = 0.8$  and  $p_{\bar{e}} = -0.6$  in the right frame of Fig.4 and find that the relevant top partner production cross sections can be enhanced by the polarized beams.

#### IV. SIGNAL AND DISCOVERY POTENTIALITY

Take into account the relatively large production cross section, we will perform the Monte Carlo simulation and explore the sensitivity of T-odd top partner production in the following section. The T-odd top partner  $T_-$  has a simple decay pattern, which decays almost 100% into the  $A_H t$  mode. We will explore the sensitivity of T-odd top partner pair production with unpolarized beam through the channel,

$$e^+e^- \rightarrow T_- \bar{T}_- \rightarrow t(\rightarrow l^+ \nu_l b) \bar{t}(\rightarrow l^- \bar{\nu}_l \bar{b}) A_H A_H \rightarrow l^+ l^- + 2b + \cancel{E}_T \quad (16)$$

which implies that the events contain one pair of oppositely charged leptons  $l^+ l^-$  ( $l = e, \mu$ ) with high transverse momentum, two high transverse momentum  $b$ -jets and large missing transverse energy  $\cancel{E}_T$ .

The dominant background arises from  $e^+e^- \rightarrow t\bar{t}$  in the SM. Besides, the most relevant backgrounds come from  $t\bar{t}Z(\rightarrow \nu\bar{\nu})$ ,  $W^+(\rightarrow l^+ \nu_l)W^-(\rightarrow l^- \bar{\nu}_l)Z(\rightarrow b\bar{b})$  and  $W^+(\rightarrow l^+ \nu_l)W^-(\rightarrow l^- \bar{\nu}_l)H(\rightarrow b\bar{b})$ . Here, the backgrounds  $ZZZ$ ,  $ZZH$  and  $ZHH$  are neglected due to their small cross sections. We turn off the parton-level cuts and generate the signal and background events by using **MadGraph 5**[30], where the **UFO**[31] format of the **LHT** model has been obtained by **FeynRules**[32] in Ref.[10]. We use **MadGraph 5** to generate the process by issuing the following commands:

generate e- e+ > thodd thodd~, (thodd > t ah, t > l+ vl b ), (thodd~ > t~ ah, t~ > l- vl~ b~ ) [for signal];

generate e- e+ > t t~, t > l+ vl b, t~ > l- vl~ b~ [for  $t\bar{t}$ ];

generate e- e+ > t t~ z, t > l+ vl b, t~ > l- vl~ b~, z > vl vl~ [for  $t\bar{t}Z$ ];

generate e- e+ > w- w+ z, w- > l- vl~, w+ > l+ vl, z > b b~ [for  $WWZ$ ];

generate e- e+ > w- w+ h, w- > l- vl~, w+ > l+ vl, h > b b~ [for  $WWH$ ].

The parton shower and hadronization are performed with `PYTHIA`[33], and the fast detector simulations are performed with `Delphes`[34]. We use the default card (i.e. `delphes_card_ILD`) of ILC in `Delphes 3.3.3`. The  $b$ -jet tagging efficiency is taken as default value in `delphes`, where it is parameterized as a function of the transverse momentum and rapidity of the jets. When generating the parton level events, we assume  $\mu_R = \mu_F$  to be the default event-by-event value. `FastJet`[35] is used to define jets via the anti- $k_t$  algorithm [36] with distance parameter  $\Delta R = 0.4$ . We use `MadAnalysis 5` [37] for analysis, where the (mis)tagging efficiencies and fake rates are assumed to be their default values.

Take into consideration the constraints on the top partner mass from current measurements, we take  $f = 700\text{GeV}$ ,  $R = 1$  (correspond to  $m_{T_-} = 708\text{ GeV}$ ) and  $f = 700\text{GeV}$ ,  $R = 1.5$  (correspond to  $m_{T_-} = 603\text{ GeV}$ ) for two benchmark points in the following calculations. In order to reduce the background contribution and enhance the signal contribution, some cuts of kinematic distributions are needed. In Fig.5, we show the normalized distributions of transverse momentum  $p_T^{l_1}$ , the pseudorapidity  $\eta_{l_1}$ ,  $\eta_{b_1}$ , the separation  $\Delta R(l_1, b_1)$  between  $l_1$  and  $b_1$ , the energy  $E(b_1 l_1)(= E(b_1) + E(l_1))$  and the total transverse energy  $H_T$ .

Since the dominant background arises from  $t\bar{t}$ , the cuts that are chosen to suppress the backgrounds should centered around the  $t\bar{t}$  background. Firstly, we can apply the cuts of general kinematic distributions, such as  $p_T^{l_1}$ ,  $\eta_{l_1}$ ,  $\eta_{b_1}$  to suppress the backgrounds. For the the  $\Delta R(l_1, b_1)$  distribution, there are two peaks in the  $t\bar{t}$ ,  $t\bar{t}Z$  backgrounds and one peak in the  $WWZ$ ,  $WWH$  backgrounds, we can use the deviation between the signal peak and background peak to suppress the backgrounds. Then, in view of the energy  $E(b_1 l_1)$  distribution, we can also use the deviation between the signal peak and background peak to reduce the backgrounds. After that, the  $H_T$  distribution of the signal can be utilized to remove the  $t\bar{t}$  background effectively. According to the above analysis, events are selected

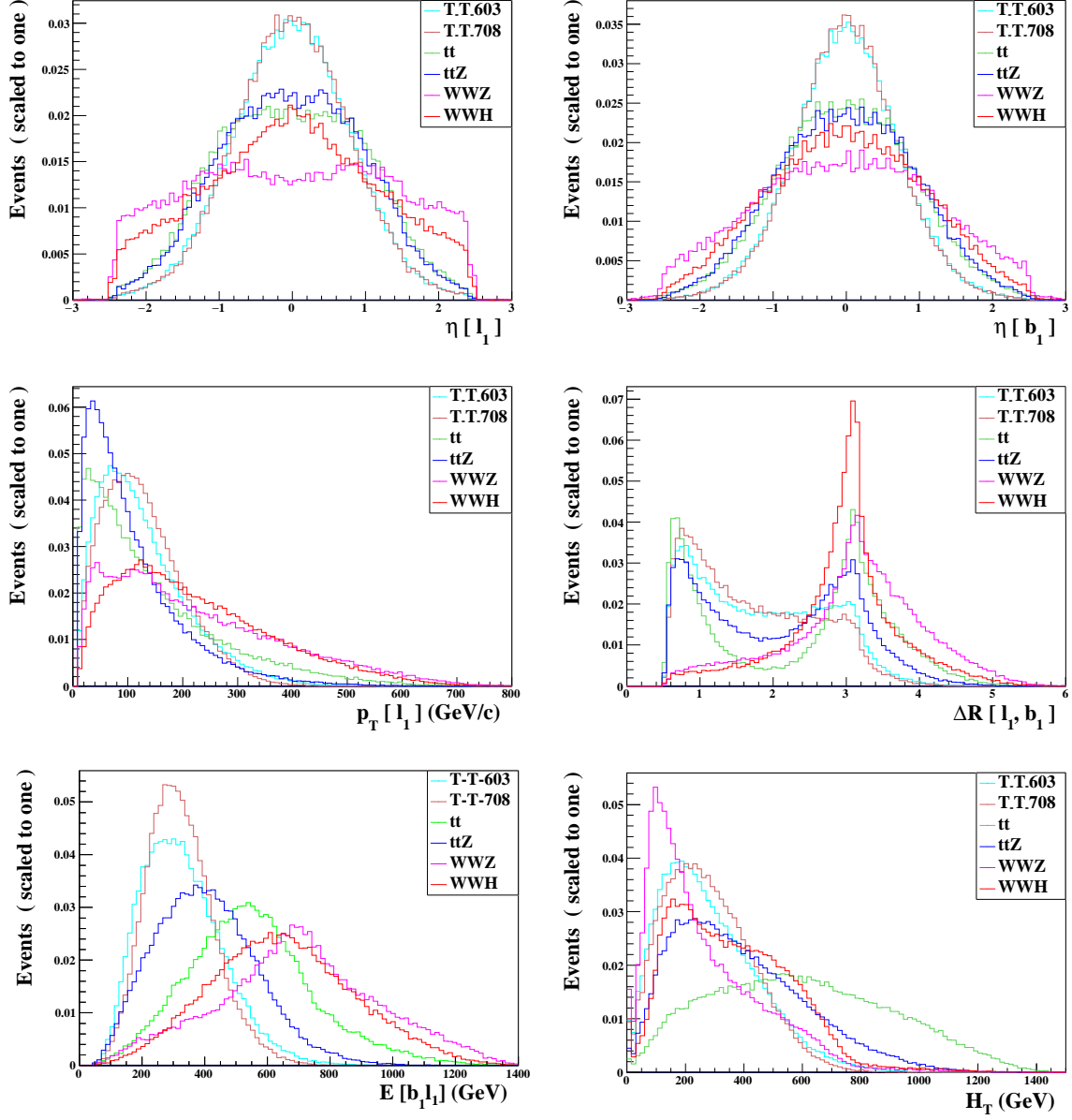


FIG. 5: Normalized distributions of  $\eta_{l_1}$ ,  $\eta_{b_1}$ ,  $p_T^{l_1}$ ,  $\Delta R_{l_1 b_1}$ ,  $E(b_1 l_1)$ ,  $H_T$  in the signal and back-grounds for the two signal benchmark points at  $\sqrt{s} = 1.5$  TeV.

to satisfy the following cuts:

$$\text{Cut-1 : } p_T(l_1) > 50\text{GeV};$$

$$\text{Cut-2 : } |\eta(l_1)| < 1; |\eta(b_1)| < 1;$$

$$\text{Cut-3 : } \Delta R(l_1, b_1) < 2.5;$$

$$\text{Cut-4 : } E(b_1 l_1) < 400\text{GeV};$$

$$\text{Cut-5 : } H_T < 400\text{GeV};$$

TABLE I: Cut flow of the cross sections for the signal(S) and the backgrounds(B) for the two signal benchmark points (P1:  $f = 700$  GeV,  $R = 1$ ) and (P2:  $f = 700$  GeV,  $R = 1.5$ ) at  $\sqrt{s}=1.5\text{TeV}$ .

Cuts	S( $\times 10^{-3}\text{fb}$ )		B( $\times 10^{-3}\text{fb}$ )				S/B	
	$T_-\bar{T}_-$ (P1)	$T_-\bar{T}_-$ (P2)	$t\bar{t}$	$t\bar{t}Z$	$WWZ$	$WWH$	P1	P2
No cut	184	119	3485	32	367	100	0.046	0.03
Cut-1	139.8	94.0	2011	20.8	283	104	0.058	0.039
Cut-2	81.1	54.9	929.6	9.6	59.8	41.1	0.078	0.053
Cut-3	62.4	45.6	334.7	5.6	15.6	11.5	0.17	0.12
Cut-4	48.7	36.5	120.1	3.4	3.0	2.2	0.38	0.28
Cut-5	44.8	33.6	34.8	2.4	2.6	1.5	1.08	0.81

For easy reading, we summarize the cut-flow cross sections of the signal and backgrounds for c.m. energy  $\sqrt{s}=1.5$  TeV in Table I. To estimate the observability quantitatively, the Statistical Significance ( $SS$ ) is calculated after final cut by using Poisson formula[38]

$$SS = \sqrt{2L \left[ (S + B) \ln \left( 1 + \frac{S}{B} \right) - S \right]}, \quad (17)$$

where  $S$  and  $B$  are the signal and background cross sections and  $L$  is the integrated luminosity. The results for the  $SS$  values depending on the integrated luminosity for  $\sqrt{s}=1.5\text{TeV}$  are shown in Fig.6. It is clear from Fig.6 that we can obtain the  $2\sigma$  significance at a luminosity of 110(200)  $\text{fb}^{-1}$  and  $3\sigma$  significance at a luminosity of 250(400)  $\text{fb}^{-1}$  for  $m_{T_-}=603(708)\text{GeV}$ .

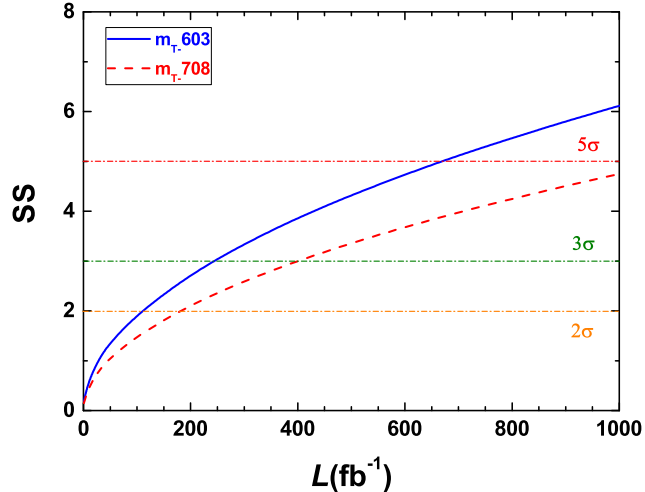


FIG. 6: The statistical significance depending on integrated luminosity for  $\sqrt{s}=1.5\text{TeV}$ .

## V. CONCLUSIONS

In this paper, we discuss the top partner production at future  $e^+e^-$  collider in the LHT model. We first consider the constraints on the top partner masses from the current measurements, then calculate the cross sections of various top partner production processes, which includes  $e^+e^- \rightarrow T_+\bar{T}_+$ ,  $e^+e^- \rightarrow T_-\bar{T}_-$ ,  $e^+e^- \rightarrow t\bar{T}_+$  and  $e^+e^- \rightarrow T_+\bar{T}_+H$ ,  $e^+e^- \rightarrow T_-\bar{T}_-H$  and  $e^+e^- \rightarrow t\bar{T}_+H$ . Next, we investigate the observability of the T-odd top partner pair production through the process  $e^+e^- \rightarrow T_-\bar{T}_- \rightarrow t\bar{t}A_H A_H$  with the di-lepton decay of the top quark pair for  $\sqrt{s}=1.5\text{TeV}$ . We display the signal significance depending on the integrated luminosity and find that the  $2\sigma$  significance can be obtained at a luminosity of 110(200)  $\text{fb}^{-1}$  for  $m_{T_-}=603(708)\text{GeV}$ , which is promising at the future high energy  $e^+e^-$  collider with high luminosity.

### Conflicts of interest

The authors declare that there is no conflict of interest regarding the publication of this paper.

## Acknowledgement

This work is supported by the National Natural Science Foundation of China (NNSFC) under grants No. 11405047, No.11404099, by the Startup Foundation for Doctors of Henan Normal University under Grant No. qd15207.

- 
- [1] G. Aad et al. [ATLAS Collaboration], Phys. Lett. B 716, 1 (2012); S. Chatrchyan et al. [CMS Collaboration], Phys. Lett. B 716, 30 (2012).
  - [2] R. Barbieri, A. Pomarol, R. Rattazzi, A. Strumia, Nucl. Phys. B 703, 127-146 (2004); Z. Han, W. Skiba, Phys. Rev. D 71, 075009 (2005).
  - [3] H. -C. Cheng and I. Low, JHEP 0309, 051 (2003); JHEP 0408, 061 (2004); I. Low, JHEP 0410, 067 (2004).
  - [4] G. Aad et al. [ATLAS Collaboration], JHEP 1411, 104 (2014); The ATLAS collaboration [ATLAS Collaboration], ATLAS-CONF-2015-012, ATLAS-COM-CONF-2015-012; S. Chatrchyan et al. [CMS Collaboration], Phys. Lett. B 729, 149 (2014).
  - [5] G. Aad et al. [ATLAS Collaboration], Phys. Rev. Lett. 108, 041805 (2012).
  - [6] J. Hubisz and P. Meade, Phys. Rev. D 71, 035016 (2005); J. Hubisz, P. Meade, A. Noble and M. Perelstein, JHEP 0601, 135 (2006).
  - [7] C. X. Yue and W. Wang, Nucl. Phys. B 683, 48 (2004); X. F. Han, Phys. Rev. D 80, 055027 (2009); B. Yang, X. Wang and J. Han, Nucl. Phys. B 847, 1 (2011).
  - [8] W. -j. Huo and S. -h. Zhu, Phys. Rev. D 68, 097301 (2003); A. J. Buras, A. Poschenrieder and S. Uhlig, Nucl. Phys. B 716, 173 (2005); J. Hubisz, S. J. Lee and G. Paz, JHEP 0606, 041 (2006); M. Blanke, A. J. Buras, A. Poschenrieder, C. Tarantino, S. Uhlig and A. Weiler, JHEP 0612, 003 (2006); A. J. Buras, A. Poschenrieder, S. Uhlig and W. A. Bardeen, JHEP 0611, 062 (2006); M. Blanke, A. J. Buras, A. Poschenrieder, S. Recksiegel, C. Tarantino, S. Uhlig and A. Weiler, JHEP 0701, 066 (2007); G. Cacciapaglia, A. Deandrea, L. Panizzi, N. Gaur, D. Harada and Y. Okada, JHEP 1203, 070 (2012); M. Blanke, A. J. Buras and S. Recksiegel, Eur.Phys.J. C 76, no.4, 182 (2016).
  - [9] M. Chala, Phys.Rev. D 96, 015028 (2017).

- [10] J. Reuter, M. Tonini and M. de Vries, JHEP 1402, 053 (2014).
- [11] J. Reuter and M. Tonini, JHEP 1302, 077 (2013); J. Berger, J. Hubisz and M. Perelstein, JHEP 1207, 016 (2012); B. F. Yang, G. F. Mi and N. Liu, JHEP 1410, 47 (2014); C. C. Han, A. Kobakhidze, N. Liu, L. Wu and B. F. Yang, Nucl. Phys. B 890, 388 (2014); X. F. Han, L. Wang, J. M. Yang and J. Y. Zhu, Phys. Rev. D 87, 055004 (2013).
- [12] G. Aarons et al., (ILC Collaboration), arXiv: 0709.1893; J. Brau et al., (ILC Collaboration), arXiv: 0712.1950; H. Baer, T. Barklow, K. Fujii et al., arXiv:1306.6352.
- [13] E. Accomando et al., (CLIC Physics Working Group Collaboration), hep-ph/0412251, CERN-2004-005; D. Dannheim, P. Lebrun, L. Linssen et al., arXiv:1208.1402; H. Abramowicz et al., (CLIC Detector and Physics Study Collaboration), arXiv:1307.5288.
- [14] A. Senol, A. T. Tasci, F. Ustabas, Nucl.Phys. B 851, 289 (2011); R. Kitano, T. Moroi, S.-F. Su, JHEP 0212, 011 (2002); Y.-B. Liu, Z.-J. Xiao, Nucl.Phys. B 892, 63-82 (2015).
- [15] K. Kong, S. C. Park, J. High Energy Phys. 0708, 038 (2007); K. Harigaya, S. Mastsumoto, M. M. Nojiri, and K. Tobioka, J. High Energy Phys. 1201, 135 (2012).
- [16] N. Arkani-Hamed, A. G. Cohen, E. Katz and A. E. Nelson, JHEP 0207, 034 (2002); N. Arkani-Hamed, A. G. Cohen, E. Katz, A. E. Nelson, T. Gregoire and J. G. Wacker, JHEP 0208, 021 (2002); I. Low, W. Skiba and D. Smith, Phys. Rev. D 66, 072001 (2002); D. E. Kaplan and M. Schmaltz, JHEP 0310, 039 (2003); S. Chang and J. G. Wacker, Phys. Rev. D 69, 035002 (2004); W. Skiba and J. Terning, Phys. Rev. D 68, 075001 (2003); S. Chang, JHEP 0312, 057 (2003); M. Schmaltz, JHEP 0408, 056 (2004).
- [17] C. R. Chen, K. Tobe and C.-P. Yuan, Phys. Lett. B 640, 263 (2006).
- [18] N. Liu, L. Wu, B. F. Yang, M. C. Zhang, Phys. Lett. B 753, 664-669 (2016); B. F. Yang, J. Z. Han and N. Liu, Phys. Rev. D 95, 035010 (2017).
- [19] [CDF Collaboration], Phys.Rev. D 88, 052013 (2013).
- [20] [D0 Collaboration], Phys. Rev. D 88, 052011 (2013).
- [21] [ATLAS Collaboration], ATL-CONF-2015-005, ATL-CONF-2015-006.
- [22] [CMS Collaboration], CMS-PAS-HIG-14-009, CMS-PAS-HIG-13-001.
- [23] P. Bechtle, S. Heinemeyer, O. Stål, T. Stefaniak, G. Weiglein, Eur.Phys.J. C 74, 2711 (2014), arXiv:1305.1933; O. Stål, T. Stefaniak, arXiv:1310.4039; P. Bechtle, S. Heinemeyer, O. Stål, T. Stefaniak, G. Weiglein, JHEP 1411, 039 (2014), arXiv:1403.1582.

- [24] P. Bechtle, O. Brein, S. Heinemeyer, G. Weiglein, K. E. Williams, *Comput. Phys. Commun.* 181:138-167,2010, arXiv:0811.4169; *Comput. Phys. Commun.* 182, 2605-2631(2011), arXiv:1102.1898; P. Bechtle, O. Brein, S. Heinemeyer, O. Stål, T. Stefaniak, G. Weiglein, K. Williams, *PoS CHARGED 2012*, 024 (2012), arXiv:1301.2345; *Eur.Phys.J. C* 74, 2693 (2014), arXiv:1311.0055; P. Bechtle, S. Heinemeyer, O. Stål, T. Stefaniak, G. Weiglein, *Eur.Phys.J. C* 75, 421 (2015), arXiv:1507.06706.
- [25] J. R. Espinosa, C. Grojean, M. Muhlleitner, M. Trott, *JHEP* 1205, 097 (2012); *JHEP* 1212, 045 (2012); P. P. Giardino et al., *JHEP* 1206, 117(2012), *Phys. Lett. B* 718, 469 (2012).
- [26] ATLAS, CMS Collaborations, *JHEP* 08, 045 (2016), arXiv:1606.02266.
- [27] A. Belyaev, N. D. Christensen and A. Pukhov, *Comput. Phys. Commun.* 184, 1729 (2013); A. Belyaev, C.-R. Chen, K. Tobe and C.-P. Yuan, *Phys. Rev. D* 74, 115020 (2006).
- [28] C. Patrignani et al., (Particle Data Group), *Chinese Physics C* Vol. 40, No. 10, 100001 (2016).
- [29] G. Moortgat-Pick et al., *Phys. Rept.* 460, 131 (2008).
- [30] J. Alwall et al., *JHEP* 07, 079 (2014).
- [31] N. D. Christensen and C. Duhr, *Comput. Phys. Commun.* 180, 1614-1641 (2009), arXiv:0806.4194.
- [32] C. Degrande, C. Duhr, B. Fuks, D. Grellscheid, O. Mattelaer, et al., *Comput. Phys. Commun.* 183, 1201-1214 (2012), arXiv:1108.2040.
- [33] T. Sjostrand, S. Mrenna and P. Z. Skands, *JHEP* 0605, 026 (2006).
- [34] J. de Favereau, et al., *JHEP* 1402, 057 (2014).
- [35] M. Cacciari, G.P. Salam and G. Soyez, *Eur.Phys.J. C* 72, 1896 (2012), [arXiv:1111.6097].
- [36] M. Cacciari, G. P. Salam, and G. Soyez, *JHEP* 04, 063 (2008).
- [37] E. Conte, B. Fuks, and G. Serret, *Comput. Phys. Commun.* 184, 222 (2013).
- [38] G. Cowan, K. Cranmer, E. Gross, and O. Vitells, *Eur. Phys. J. C* 71, 1554 (2011).